Histological and Immunohistochemical Study on the Effect of Sodium iodate on the Retina of Adult Male Albino Rat and the Possible Protective Role of Silymarin

Original Article

Rania Ibrahim Yassien[1], Omyma Ibraheem Ibraheem Zedan[2] and Nagwa Saad Ghoneim[1]

[1]Department of Histology, [2]Department of Anatomy, Faculty of Medicine, Menoufia University, Egypt

ABSTRACT

Background: Retinal degenerative diseases are induced by many environmental and genetic agents and may lead to permanent blindness. Induced retinal degeneration by sodium iodate ($NaIO_3$) is widely used to study mechanism of retinal cell death. Silymarin are flavonoids which has powerful antioxidant effects.

Aim of Work: Study the effects of $NaIO_3$ on the retina of adult male albino rat and possible protective role of silymarin.

Material and Methods: Forty adult male albino rats were used, they were divided equally to four groups: group I (control), group II (silymarin), group III ($NaIO_3$) and group IV (silymarin and $NaIO_3$). At end of experiment, retina of the whole groups was prepared for histological and immunohistochemical studies. Paraffin sections were stained by hematoxylin and eosin (H&E), Glial fibrillary acidic protein (GFAP), Caspase3 and inducible nitric oxide synthase (iNOS) immunostaining. Morphometric measurements were done and data was statistically analyzed.

Results: H &E sections of GIII revealed thinning, disorganization and loss of most layers of retina. Degeneration of retinal pigmented epithelium, damage of photoreceptors, necrosis and loss of cells of outer, inner nuclear layers and ganglion cell layers were noticed. Loss of reticular appearance, thinning of outer and inner plexiform layers and congested blood vessels in many layers were detected. GFAP, Caspase3 and iNOS revealed strong positive immune reaction in this group. Group IV showed marked improvement of retina but some changes were still seen. Electron microscope (EM) and morphometric results confirmed light microscopic results.

Conclusion: Sodium iodate has destructive effects on all layers of retina and preceding silymarin has protective role.

Received: 14 October 2020, **Accepted:** 05 December 2020

Key Words: EM, $NaIO_3$, retina, silymarin.

Corresponding Author: Rania Ibrahim Yassien, PhD, Department of Histology, Faculty of Medicine, Menoufia University, Shebin el Kom, Egypt, **Tel.**: +201 028073793, **E-mail:** raniayassien@yahoo.com

ISSN: 1110-0559, Vol. 44, No.4

INTRODUCTION

World-wide retinal diseases such as glaucoma, age related macular degeneration, diabetic retinopathy, retinitis pigmentosa and other degenerative retinal diseases that finally end in blindness are evaluated to affect more than 12% of patients over the age of 40[1].

Retinal degenerative diseases are induced by many environmental and genetic agents which lead to permanent blindness even in developed nations. Although, these diseases have different pathological pathways, but the resulting degeneration have almost the same pictures[2].

Nowadays, many researches have been performed to improve various degrees of irreversible loss of vision of millions of patients around the world[3].

Induced retinal degeneration by sodium iodate ($NaIO_3$) is widely used to study mechanisms of cell-death in retina[4]. $NaIO_3$ is a stable oxidizing compound which is especially toxic for retina. This toxicity is proved in many various mammalian kinds, as sheep, rabbit, rat and mouse[5]. Sodium iodate is reported to induce both retinal necrosis and apoptosis[6]. $NaIO_3$ may affect retinal pigment epithelium (RPE) firstly with following damage to sensory retina or it directly affect function and structure of the whole retina[7].

Retinal damage could be induced from oxidative stress by sodium iodate. Also, some reports support that $NaIO_3$ denatures retinal proteins containing sulfhydryl group and decreases activity of sulfhydryl containing enzymes. Furthermore, melanin presents in retina make the cells more sensitive to $NaIO_3$[8].

The retina is extremely threatened by oxidative stress due to elevated metabolism, high exposure to light and elevated content of lipofuscin[9].

The retinal pigment epithelium (RPE) has several significant functions in the maintenance of visual clarity of the eye[10]. RPE cells transfer nutrients and metabolites to the neuroretina, recycle retinoids, storing vitamin A and its pigments absorb excess light[8]. Additionally, RPE engulfs

 DOI: 10.21608/ejh.2020.46113.1373

metabolic waste and phagocytoses shed photoreceptor segments[11].

Reaching new drugs for preventing and enhancing retinal degeneration with less toxicity and more efficacy with understanding their mechanisms are important[12].

Natural flavonoids which have antioxidants effects, are commonly present in natural plants. It is helpful in reducing and hindering the development of retinal degeneration[9].

Silymarin flavonoid is derived from silybummarianum. It has antioxidant effects for various toxicities[13].

Silymarin high doses has a good safety profile with no adverse side effects in humans and animals. It is used mainly in liver disease. But, lately, Silymarin has been described to be an effective neuroprotective factor against many neurodegenerative disorders including Alzheimer's disease, Parkinson's disease and cerebral ischemia[14].

The neuroprotective effect of silymarin appears to be unique because it has antioxidant, anti-amyloidogenic, anti-inflammatory, and pro-estrogenic properties. Silymarin elicits its neuroprotective effects by reducing both lipid and protein oxidation, as well as by activating acetylcholinesterase activity and suppress inducible nitric oxide synthase gene expression[14]. Although $NaIO_3$ has been used for evaluation of retinal toxicity, its effect remains poorly characterized so, this research is aimed to estimate $NaIO_3$ effects on the retina and the possible protective role of Silymarin.

MATERIALS AND METHODS

Animals

This study was carried out on 40 adult male albino rats weighing 200-250 g.

Animals were housed in clean properly ventilated cages, fed on a standard laboratory diet, and maintained on a12-h light/dark photoperiod in the animal house of the Faculty of Medicine, Menoufia University, Shebin el Kom, Menoufia, Egypt. This experiment was done according to the Animal Care and Ethical Committee Guidelines of the Faculty of Medicine, Menoufia University.

Chemicals and drugs

$NaIO_3$ (Sigma-Aldrich Corp., St. Louis, MO, USA) was dissolved in saline. Each 400 mg NaIo3 was dissolved in 50 ml 0.9 % saline.

Silymarin (Sedico Arabic company) was dissolved in dimethyl sulfoxide (DMSO). Each 1000 mg Silymarin was dissolved in 20 ml 0.1% DMSO.

We divided rats randomly into four equal groups:

Group I (control group): included 10 rats which then subdivided equally into:

o subgroup Ia (5 rats): injected by 1ml saline/ each rat (200 g) through a tail vein daily for 7 days.

o subgroup Ib (5 rats): received 1ml DMSO / each rat (200g) orally by gastric tube daily for 3 months.

Group II (silymarin): included 10 rats that received 250mg/kg silymarin (each rat weighing 200mg was received 1ml DMSO contained 50 mg Silymarin) orally by gastric tube daily for 3 months[13].

Group III ($NaIO_3$): included 10 rats that were injected with 40 mg/kg of $NaIO_3$ (each rat weighing 200 mg was received 1ml saline contained 8mg $NaIo_3$) through a tail vein daily for 7 days[5].

Group IV (silymarin & $NaIO_3$): included 10 rats that received silymarin orally for 3 months before starting sodium iodate injection for the same dose and duration as before.

Finally, the animals were anaesthetized using a mixture of ketamine (100 mg/mL; Hopira, Lake Forest, IL, USA) and xylazine (20 mg/mL; Akorn, Lake Forest, IL, USA) with a 2:1 volume ratio[15] then both eyes were enucleated. The right eyeballs were injected with formalin for light microscopic study and the left ones were injected with 5% phosphate buffered glutaraldehyde for electron microscopic study. The posterior part of the eye including the retina was preserved in the same solutions.

A. For light microscopic study: paraffin blocks were prepared from the retina and 5µm thick serial sections were obtained and stained with:

1. Hematoxylin and Eosin stain (H&E)[16].
2. Immunohistochemical staining:

a. Glial fibrillary acidic protein (GFAP) immunostaining: antibody (purchased from Bio genex, USA) was used to detect astrocytes and Muller cells in a ready to use technique. Sections were deparaffinized in xylene for one hour. Two drops of primary antibody were applied and incubated for one hour at room temperature then washed twice with phosphate buffer saline (PBS). Two drops of biotinylated secondary-antibody were applied and then incubated for 30 minutes at room temperature then washed twice with PBS. Two drops of DAB solution were applied to all sections and incubated for ten minutes[17].

b. Caspase-3 immunostaining: It was performed using the avidin–biotin peroxidase technique using a mouse monoclonal antibody (Lab Vision, USA)[18].

c. Inducible nitric oxide synthase (iNOS) immunostaining: iNOS antibody is a rabbit polyclonal antibody (Lab Vision Corporation Laboratories, catalogue number PA1-036). Immunostaining required pretreatment, this was done by boiling for 10 minutes in 10Mm citrate buffer (cat no AP 9003) pH 6 for antigen retrieval and leaving the sections to cool in room temperature for 20 minutes. Then, the sections were incubated for one hour with the primary antibodies. Immunostaining was completed by the use of Ultravision detection system (cat no TP - 015- HD)[18].

Then sections were washed in distilled water and counterstained with Mayer's hematoxylin (cat no TA-060- MH) for two minutes. Negative control sections were processed by replacing the primary antibody by PBS. Primary antibodies, citrate buffer, Ultravision detection system and Mayer's hematoxylin were purchased from Labvision Thermoscientific USA[18].

B. For transmission electron microscope: Tissue samples from 4 rats were randomly chosen in each group. Small biopsies from the retinas of the sacrificed animals were excised rapidly (within 1 min) and trimmed into about 1x1 mm^2 pieces. Specimens were processed for semithin sections (1μm thick). Ultrathin sections were examined with transmission electron microscope (Seo-Russia) in Tanta E.M Center, Faculty of Medicine, Tanta University[19].

Morphometric and statistical study

The mid-center region of the retina in five different stained sections from five different rats were examined in each group (five high power fields /section) to measure:

a. The mean thickness of outer nuclear layer (ONL).
b. The mean thickness of outer plexiform layer (OPL).
c. The mean thickness of inner nuclear layer (INL).
d. The mean thickness of inner plexiform layer (IPL).
e. The mean of the numbers of ganglion cells.
f. The mean area percentage of GFAB positive immune reaction.
g. The mean area percentage of caspase-3 positive immune reaction.
h. The mean area percentage of iNOS positive immune reaction.

The measurements were done by using the image analyzer (Leica Q 500 MC program, Wentzler, Germany) in the Anatomy Department, Faculty of Medicine, Menoufia University.

Morphometric data were statistically analyzed using SPSS (Statistical Package for the Social Sciences) program, version 17, (IBM Corporation, Somers, New York, USA). The data was presented as mean ± SEM (standard error of mean). The mean of each group was compared with that of the control using one-way analysis of variance (ANOVA) then "Turkey" post hoc test. When *P value* was < 0.05, results were considered significant and *P value* was < 0.001, results were considered highly significant[20].

RESULTS

Light microscopic results

A) Hematoxylin and Eosin results

(H & E) stained sections of retina of control group (GI) and silymarin group (GII) showed from choroid to vitreous body, the retinal pigmented epithelium (RPE) which appeared as single row of low cuboidal cells with flattened nuclei (Figure 1). The photoreceptor layer (PRL) formed of outer and inner segments of rod and cone cells. The outer limiting membrane (OLM) appeared as dark continuous line between inner segment of photoreceptor cells and outer nuclear layer. The outer nuclear layer (ONL) formed of densely packed nuclei of rod and cone cells and thin outer plexiform layer (OPL) with reticular appearance between outer and inner nuclear layers were seen. The (INL) inner nuclear layer nuclei appeared larger and paler in comparison to outer nuclear layer. The inner plexiform layer (IPL) with reticular appearance appeared thicker than outer plexiform layer. The ganglion cell layer (GCL) formed of large, rounded, variable sized and separated cells with pale nuclei. The nerve fiber layer (NFL) composed of axons of ganglion cell layer. The inner limiting membrane (ILM) appeared as dark continuous line separating retina from vitreous body (Figures 2,3).

H&E stained sections of sodium iodate group (GIII) showed choroid with dilated congested blood vessels which surrounded by cellular infiltration. Degeneration of retinal pigmented epithelium and photoreceptor layers was seen. Some RPE cells appeared with pyknotic nuclei. RPE appeared detached from neuroretina. (Figure 4). Thinning, degeneration and cytoplasmic vacuolation of ONL, INL, GCL and NFL were detected. Disorganized ganglion cells were detected. Disrupted ILM was noticed (Figure 5). Loss of reticular appearance and deposition of esinophilic material in OPL was seen. Pyknotic nuclei of INL and GCL cells were seen (Figures 5,6).

Thin irregular choroid ,loss of RPE and PRL ,thinning and disorganization of cells of ONL and INL were seen. Marked narrowing OPL and IPL with disorganized cells and loss of reticular appearance were detected. GCL showed deposition of eosinophilic material (Figure 6).

Apparent thinning of the all layer of retina with loss of cells were detected. Degenerated INL cells, vacuolation of INL and IPL and abnormal cells in IPL were seen. Some GCL cells with pyknotic nuclei were detected. Dilated congested blood capillaries appeared in ONL & GCL and also, hemorrhage was seen in ONL (Figure 7).

H&E stained sections of group IV showed marked improvement of histological picture and appearance of all layers of retina but few vacuolation in ONL and INL and some cells in IPL were still seen (Figure 8).

B) Immune histochemical results

A) Glial Fibrillary acid protein (GFAP) stain

GFAP stained sections of retina of (GI) and (GII) revealed positive immune reaction of astrocyte in GCL and NFL only (Figures 9,10). Sections of (GIII) showed strong positive immune reaction of Muller cells INL with extension of thick processes to IPL. Strong positive reaction of astrocytes in GCL and NFL and around blood vessels were seen. (Figure 11). Group IV revealed positive

reaction of astrocyte in GCL and NFL. But weak reaction of Muller cells in ONL with extension of thin processes to OPL was also seen. (Figure 12)

B) Caspase-3 stain

Caspase-3 stained sections of retina of (GI) and (GII) showed negative caspase immune reaction in all layers of retina (Figure 13). Sections of (GIII) showed strong positive immune reaction in ONL, INL and GCL with some positive reaction of all other layers (Figure 14). Sections of (GIV) revealed moderate immunoreactivity in GCL only and negative reaction in ONL and INL (Figure 15).

C) iNOS stain

iNOS stained sections of (GI) and (GII) revealed negative immunoreactivity for all layers of retina. (Figure 16). While in (GIII) strong positive immune reaction in all layers of retina was seen (Figure 17). On the other hand (GIV) showed moderate immune reaction in GCL and negative reaction in ONL and INL (Figure 18).

Electron microscopic results

By transmission electron microscope (TEM) examination, retina of the control and silymarin groups showed that the RPE cells resting on Bruch's membrane and had basal rounded to oval nuclei, basal mitochondria and basal membrane infoldings. Melanin pigments, intercellular junction and apical microvilli were seen (Figures 19,23). The outer segments (OS) of photoreceptor cells were seen as elongated, cylindrical structures containing flattened horizontal lamellar discs (Figures 20a,24a). Longitudinal cylindrical inner segments (IS) containing mitochondria and electron dense ILM were detected (Figure 24a). ONL contained cell bodies of rod and cone cells with minimal intercellular spaces. Rod nuclei were characterized by heterochromatin condensation, and surrounded by a thin rim of cytoplasm. However, cone nuclei were less heterochromatic (Figures 20b,24b). In the inner nuclear layer, horizontal cells appeared with large oval electron lucent nucleus. The nuclei of bipolar cells appeared rounded or elliptical in shape and surrounded by thin rim of cytoplasm. Muller cells contained nuclei of high density and showed numerous processes. (Figure 21). Wide IPL with terminal synaptic processes was seen (Figure 25) followed by GCL containing ganglion cells which had oval euchromatic nucleus and prominent nucleolus with irregular nuclear envelop and cytoplasm containing mitochondria, RER and dilated SER were detected. The inner limiting membrane appeared as electron dense line (Figure 22,25). NFL contained unmyelinated axons of ganglion cells was detected (Figure 22).

EM sections of retina of (GIII) showed RPE cells with irregular shrunken heterochromatic nuclei, vacuolation of cytoplasm, damaged mitochondria with destructed cisternae, irregular apical microvilli, disrupted junction complexes between cells and destructed basal infoldings (Figure 26). OS of PRL showed disorganized lamellar discs with vesicular dilatation (Figure 27). Distorted ONL with heterochromatic nuclei of its cells with vacuolation between cells. OPL appear distorted with some vacuoles. some INL cells appear distorted with destructed mitochondria and others with heterochromatic nucleus. Markedly necrotic cells and remnants of some cells with ballooned mitochondria in INL are seen (Figure 28).

OPL showed congested blood capillary (Figures 29,30) and dilated terminal synaptic processes. The INL contained bipolar, Muller cells and some necrotic cells with wide spaces in between (Figure 29). Shrunken irregular apparently increased in number Muller cells with loss of their process were detected. Rarefied cytoplasm of bipolar cells and horizontal cells were seen. Necrotic cell with multiple vacuolation between cells were detected (Figure 30)

Cells of GCL showed irregular ganglion cells with electron dense irregular nuclei. The cytoplasm of the cells contained dilated rough endoplasmic reticulum, and degenerated mitochondria. Distorted terminal synaptic process in IPL and damaged distorted inner limiting membrane were also seen (Figure 31).

EM sections of retina of (GIV) showed marked improvement but some retinal pigmented epithelium showed rarefied cytoplasm and mitochondria with irregular cristae and few melanin pigments. Few pyknotic cell were still seen (Figure 32).

OS of PRL showed horizontal lamellar discs in some area and vacuolar degeneration in others. Cells of rods and cones of ONL appeared with some space and vacuoles between them. Few necrotic cells were still seen (Figure 33).

INL showed Muller, bipolar and horizontal cells but small shrunken cells and small vacuoles were still seen (Figure 34).

Some ganglion cells showed mitochondria with irregular cristae and irregular inner limiting membrane was also seen (Figure 35).

By morphometric analysis, there was a highly significant decrease ($P< 0.001$) in both ONL, OPL, INL and IPL thickness in group III compared to control (Table 1, Chart 1). The ganglion cells number showed highly significant decrease ($P< 0.001$) as compared to control (Table 2, Chart 2).

There was a significant increase in GFAP, Caspase 3, iNOS positive immune reaction ($P< 0.05$) in group III as compared with control group (Table 3, Chart 3).

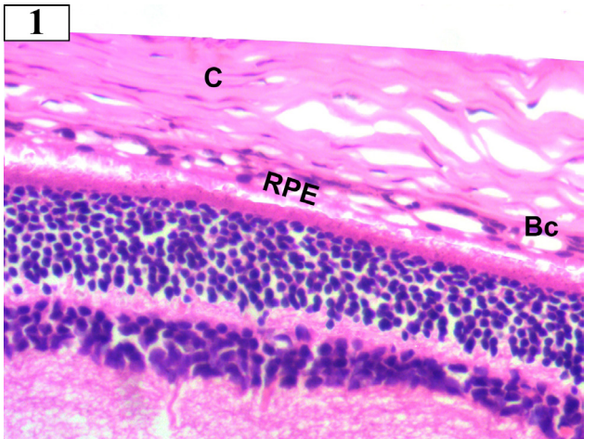

Fig. 1: H&E stained section of retina of (GI) showing RPE layer and overlying choroid (C) containing blood capillaries (Bc). (H&E X400)

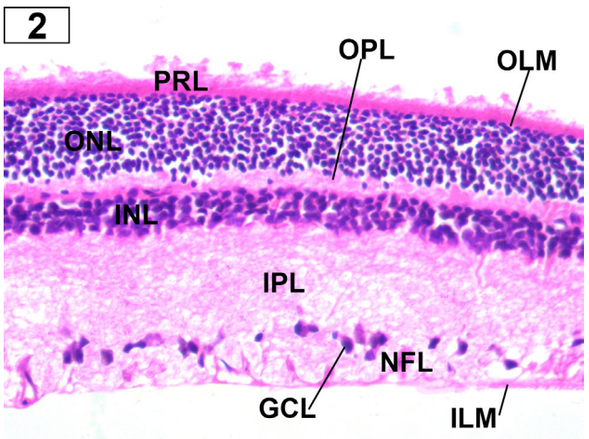

Fig. 2: H&E stained section of retina of (GI) showing PRL layer, OLM, thick ONL with densely packed nuclei of rods and cones. Thin OPL with reticular appearance, thin INL with larger and paler nuclei, thick reticular IPL, GCL with single raw of large ganglion cells, NFL layer and ILM are seen. (H&E X400)

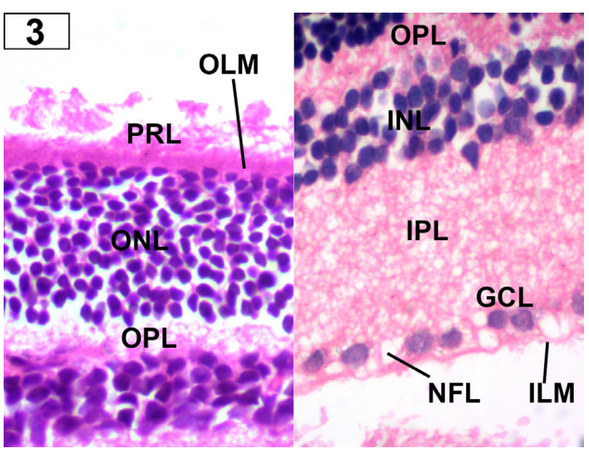

Fig. 3: H&E stained section of retina of (GII) showing all layers of retina. (H&E X400)

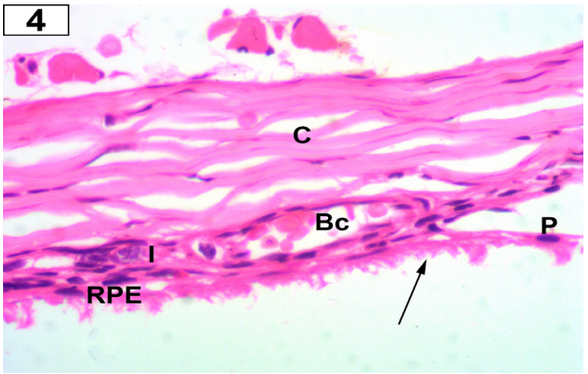

Fig. 4: H&E stained section of (GIII) showing degenerated PRL layer (arrow), some RPE cells with pyknotic nuclei (P). Dilated congested blood capillaries (Bc) and lymphocytic infiltration (I) in choroid (C) are seen. Notice: separation of RPE from sensory retina. (H&E X400)

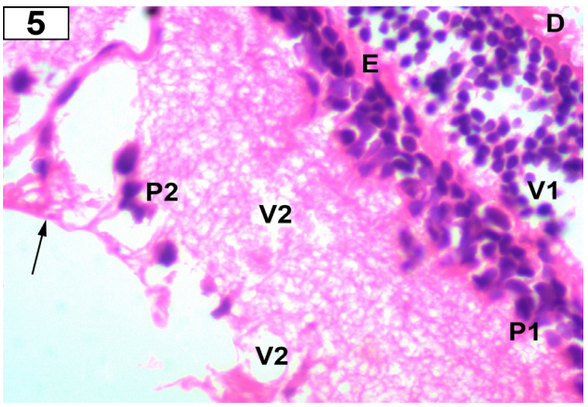

Fig. 5: H&E stained section of retina of (GIII) showing degeneration of PRL layer (D), marked vacuolation (V1) in ONL, loss of reticular appearance and deposition of esinophilic material (E) in OPL. Pyknotic nuclei (P1) of INL cells, vacuolation (V2) of IPL, GCL and NFL are seen. Disorganized ganglion cells with pyknosis (P2) are detected. Notice: disrupted ILM (arrow). (H&E X400)

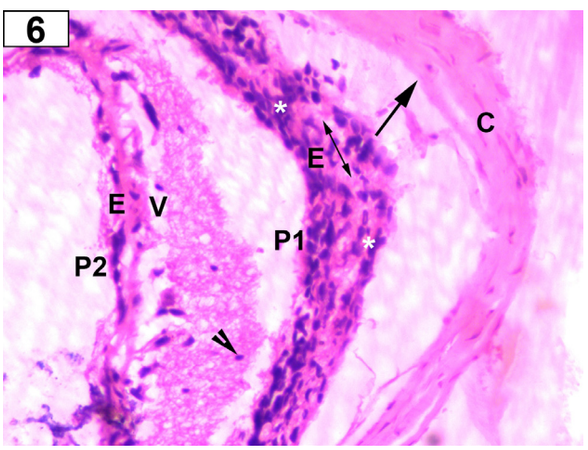

Fig. 6: H&E stained section of retina of (GIII) showing thin irregular choroid (C) loss of RPE and PRL (arrow), thinning and disorganization of cells of ONL and IN L (*) marked narrowing OPL (double heads arrow), vacuolation (V)in IPL with disorganized cells (arrow head) and loss of reticular appearance. Deposition of esinophilic material (E) in ONL and GCL. Pyknotic nuclei (P1) in INL cells and (P2) in ganglion cells are seen. (H&E X400)

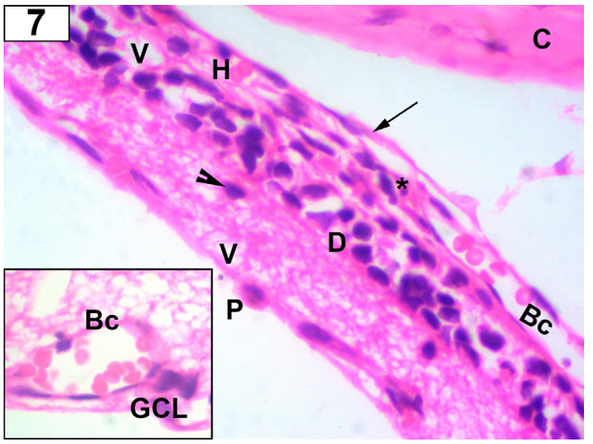

Fig. 7: H&E stained section of retina of (GIII) showing apparent thinning of the all layer of retina, loss of RPE and PRL (arrow), thin ONL (*) with loss of cells and dilated blood capillaries (Bc) and hemorrhage (H). Degenerated INL cells (D), vacuolation (V) of INL and IPL and abnormal cells in IPL (arrow head) are seen. Some GCL cells with pyknotic (P) are detected. Inset: showing congested blood capillaries (Bc) in GCL. (H & E X400)

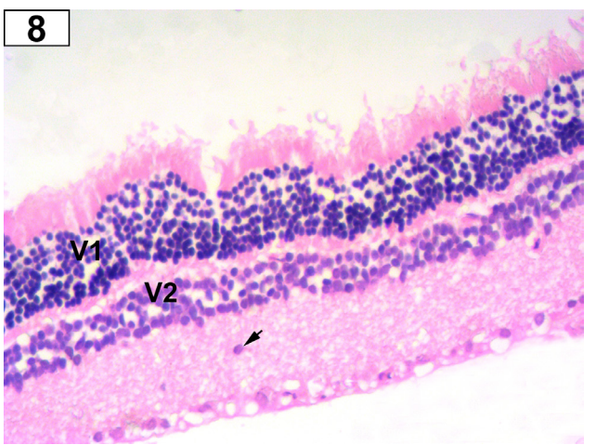

Fig. 8: H&E stained section of (G IV) showing nearly apparent normal retina with few vacuolation (V1) in ONL and (V2) in INL. Notice: some cells in IPL (short arrow) are still seen

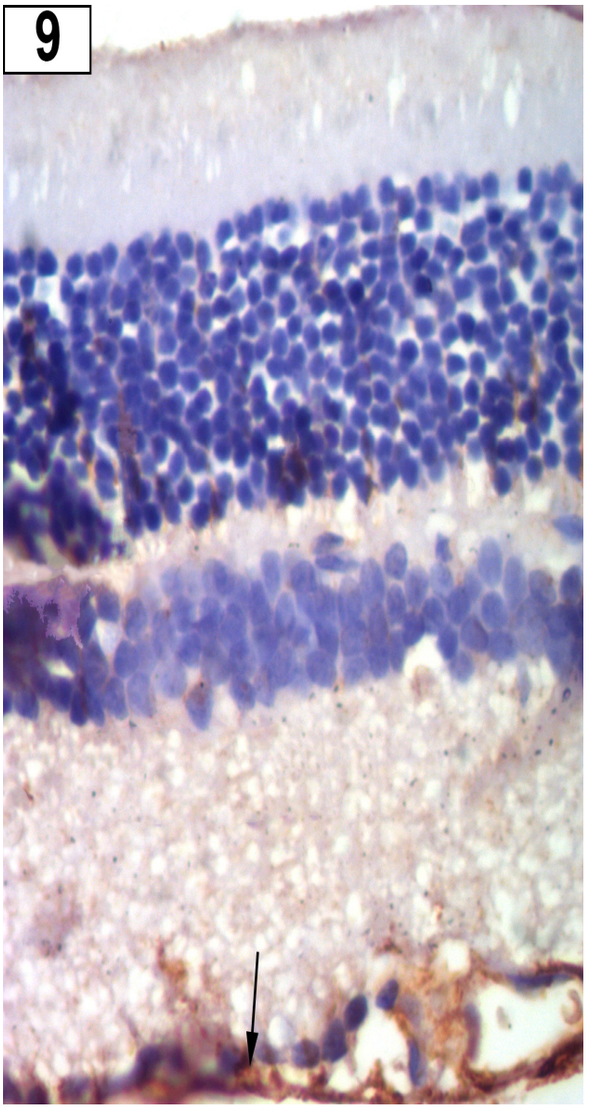

Fig. 9: GFAP stained section of retina of (GI) showing positive immune reaction to astrocyte in NFL and GCL (arrow). (GFAP X200)

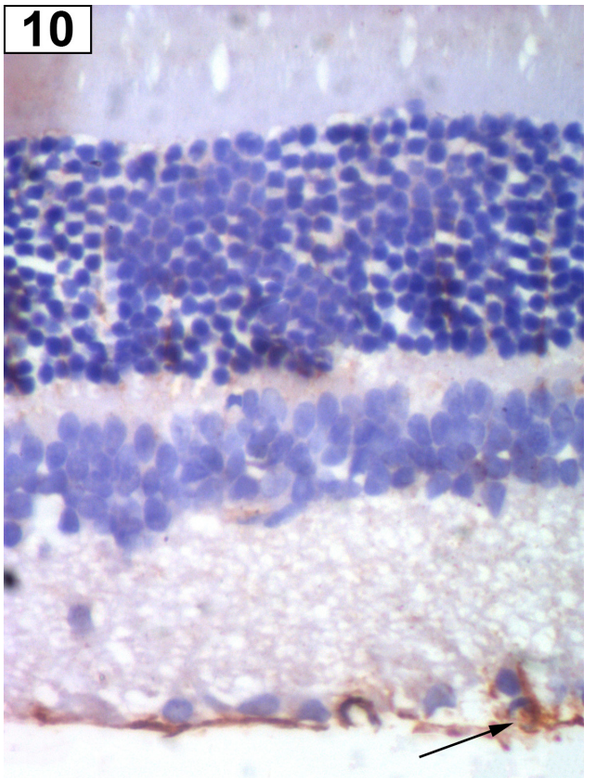

Fig. 10: GFAP stained section of retina of (G II) showing positive immune reaction of astrocyte in NFL and GCL (arrow). (GFAP x 200)

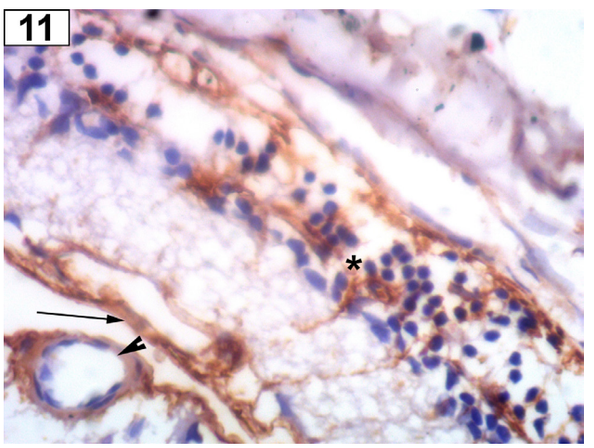

Fig. 11: GFAP stained section of retina of (GIII) showing strong positive immune reaction of muller cells in INL (*) with extension of thick process to IPL. Strong positive reaction of astrocytes in GCL and NFL (arrow) and around blood vessels (arrow head). (GFAP X200)

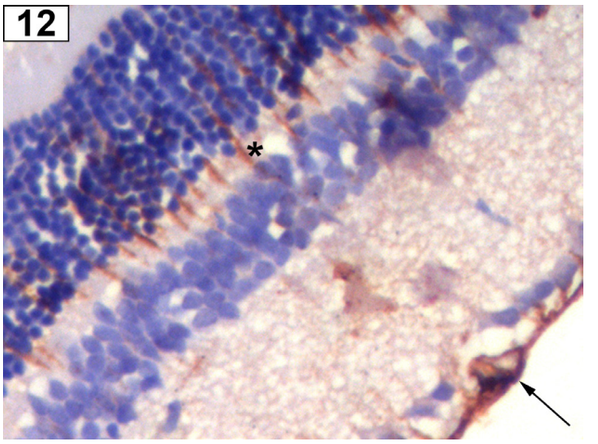

Fig. 12: GFAP stained section of retina of (G IV) showing positive immune reaction of astrocyte of GCL and NFL (arrow), weak reaction of Muller cells in ONL and extension of thin processes to OPL (*). (GFAP X200).

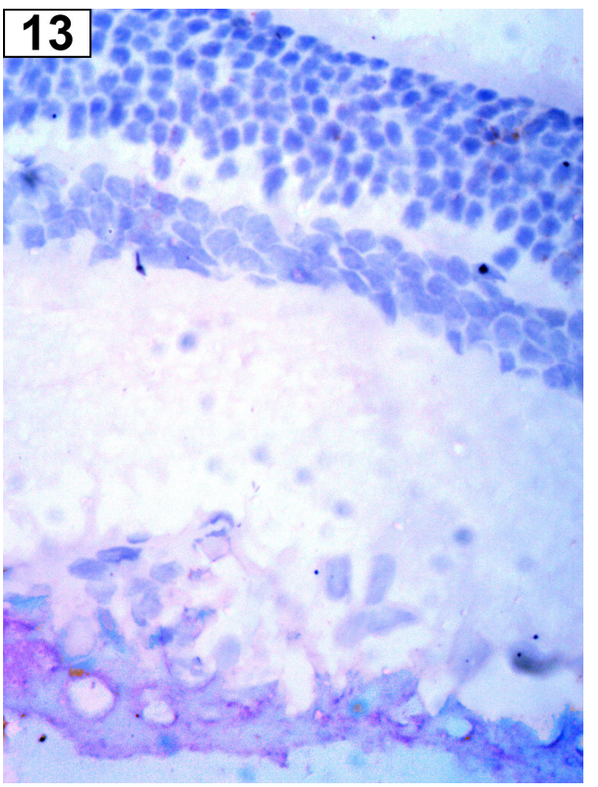

Fig. 13: Caspase-3 stained section of (GI & GII) showing negative reaction of all layers of retina. (Caspase 3 X200)

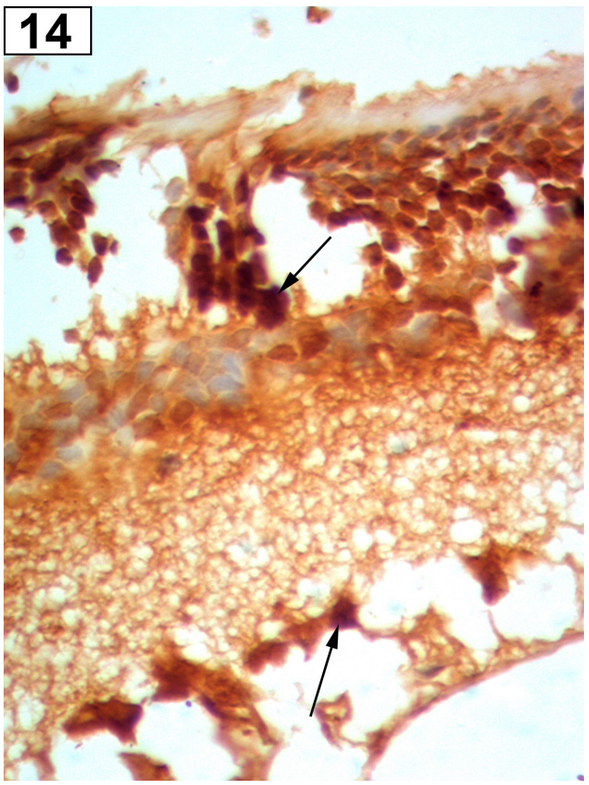

Fig. 14: Caspase-3 stained section of (G III) showing strong positive immune reaction in ONL, INL and GCL (arrows) with some positive reaction of all other layers (Caspase 3 X200)

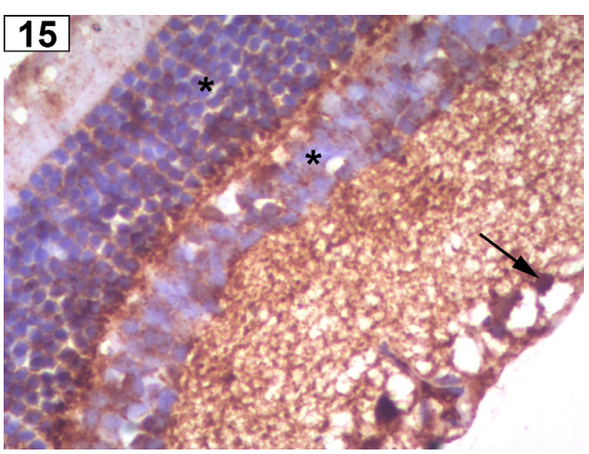

Fig. 15: Caspase-3 stained section of (GIV) showing moderate positive reaction in GCL (arrow) and negative reaction in INL &ONL (*). (Caspase-3 X200)

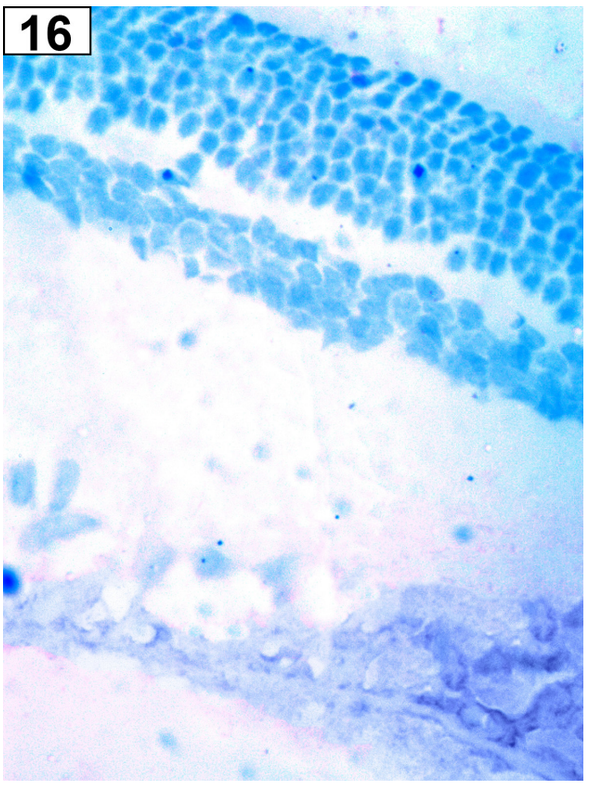

Fig. 16: iNOS stained section of (GI & GII) showing negative immune reaction in all layers of retina. (iNOS X200)

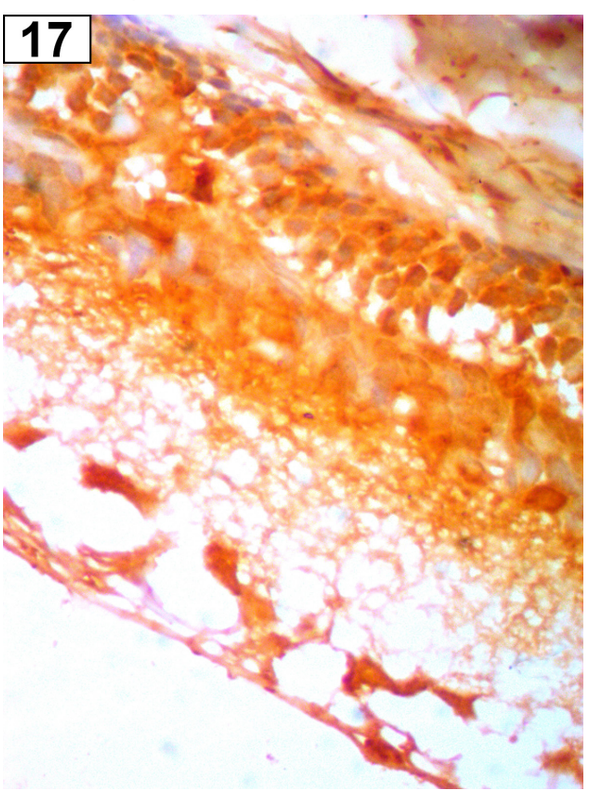

Fig. 17: iNOS stained section of (G III) showing strong positive immune reaction in all layers of retina. (iNOS X200)

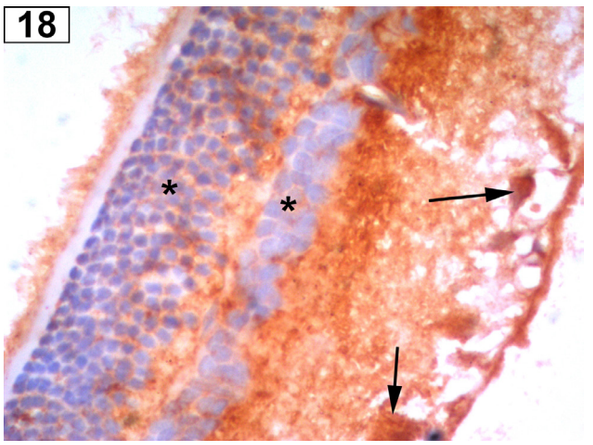

Fig. 18: iNOS stained section of retina of (G IV) showing moderate positive immune reaction in GCL (arrows) and negative reaction in ONL and INL (*). (iNOS X200)

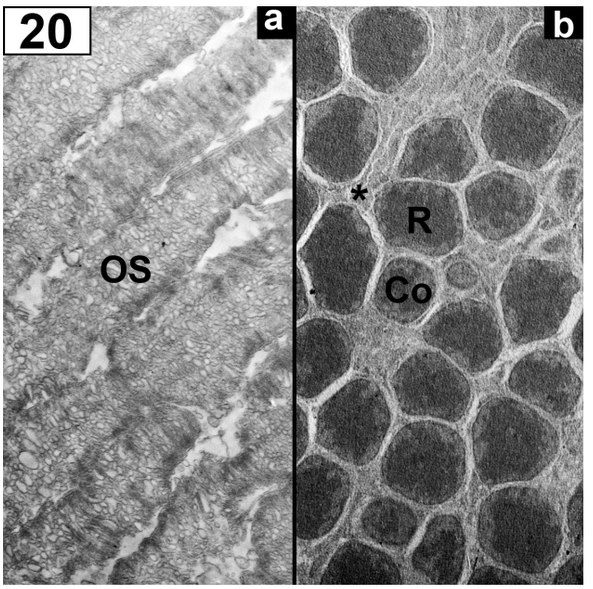

Fig. 20: EM of retina of (GI) showing (a part) outer segments (OS)of rods photoreceptors (PRL) as elongated, cylindrical structures containing flattened horizontal lamellar discs. (b part) showing rods (R) and cones (Co) cell bodies with minimal intercellular spaces (*). Rod nuclei are characterized by heterochromatin condensation, and surrounded by a thin rim of cytoplasm. However, cone nuclei are less heterochromatic.

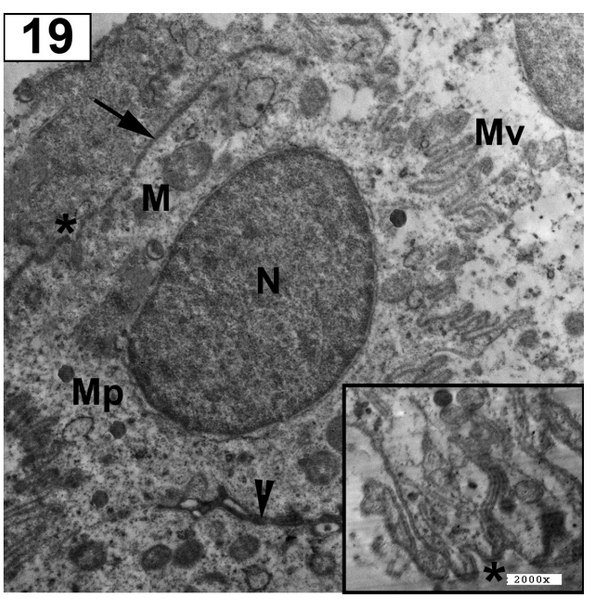

Fig. 19: E M of retina of (GI) showing retinal pigmented epithelium resting on Brush membrane (arrow) with basal membrane infoldings (*), basal mitochondria (M) and basal oval nucleus (N). Melanin pigments (Mp), intercellular junction (arrow head) and apical microvilli (Mv) are seen. Inset: marked basal infoldings in another cell

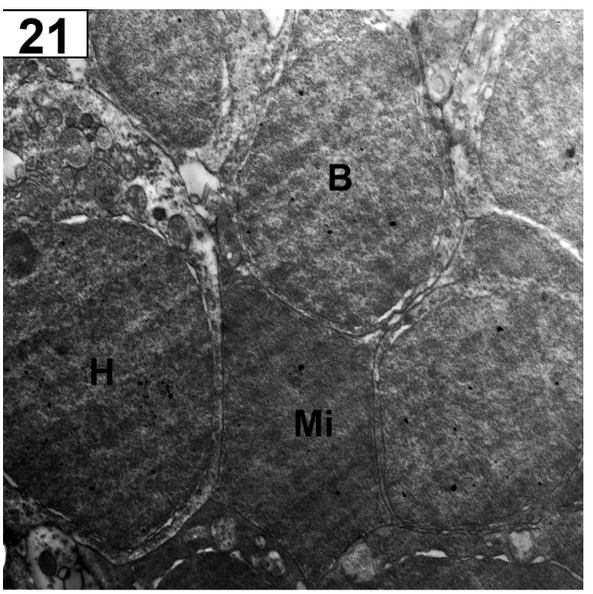

Fig. 21: EM of retina of INL of (GI) showing horizontal cells appear with large oval electron lucent nucleus (H). The nuclei of bipolar cells appear rounded or elliptical in shape and surrounded by thin rim of cytoplasm (B). Muller cells contain nuclei of high density and show numerous processes (Mi).

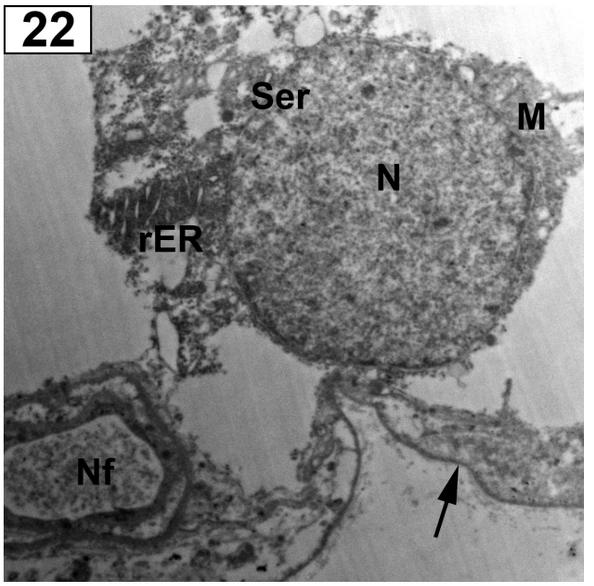

Fig. 22: E M of retina of GCL of (GI) showing a ganglion neuron with rounded euchromatic nucleus (N), mitochondria (M), regular rER and dilated SER (Ser). Nerve fiber (Nf) in NFL and the inner limiting membrane (arrow) are seen.

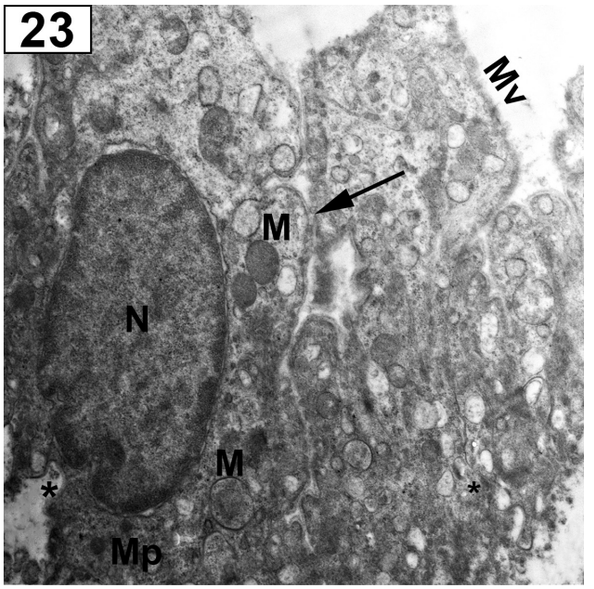

Fig. 23: EM of retina of RPE of (GII) showing oval indented nucleus (N) with numerous invaginations of the basal membrane (*) associated with mitochondria (M), melanin pigment (Mp), intercellular junction (arrow) and microvilli on the surface (Mv).

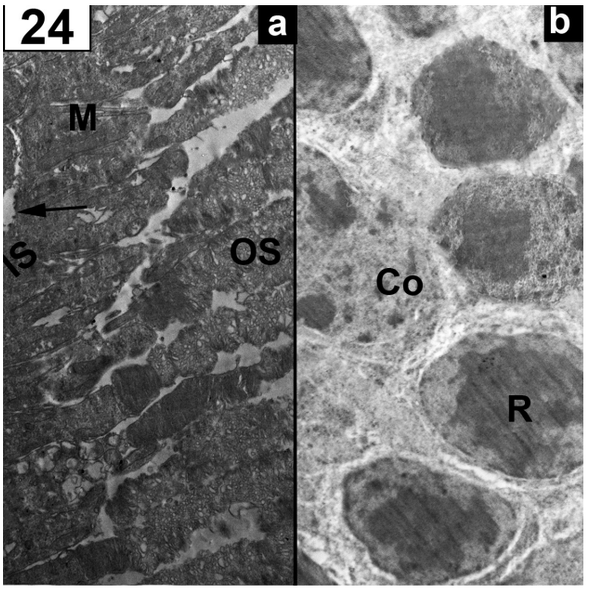

Fig. 24: EM of retina of (GII) showing (a part) outer segment (OS), inner segment (IS) with mitochondria (M) of PRL, outer nuclear membrane (arrow) and (b part) rods(R) & cones cells (Co) of ONL.

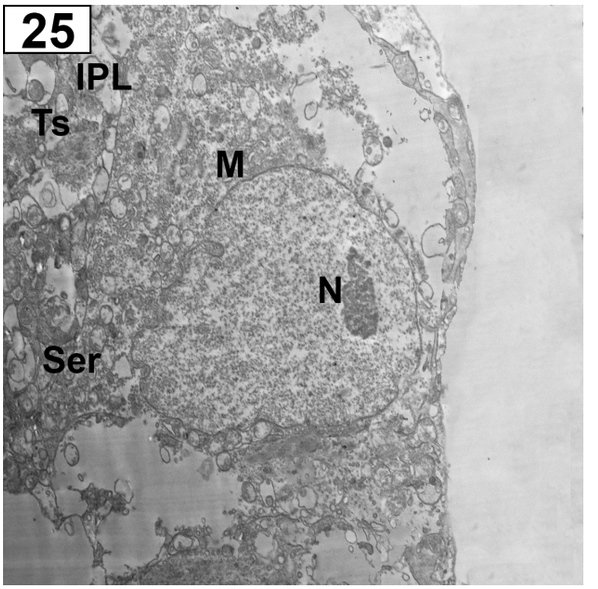

Fig. 25: EM of retina of (GII) showing a ganglion neuron with oval euchromatic nucleus (N), mitochondria (M), and (Ser). Notice: terminal synaptic processes (Ts) in the IPL.

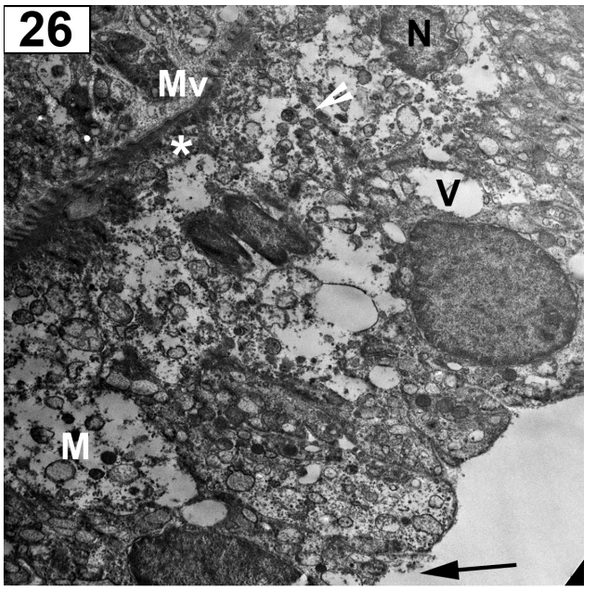

Fig. 26: EM of retina of RPE of (GIII) showing irregular shrunken heterochromatic nuclei (N), vacuolation (V) of cytoplasm, damaged mitochondria with destructed cisternae (M), irregular apical microvilli (Mv), disrupted junction complexes (arrow head) and destructed basal infoldings (arrow).

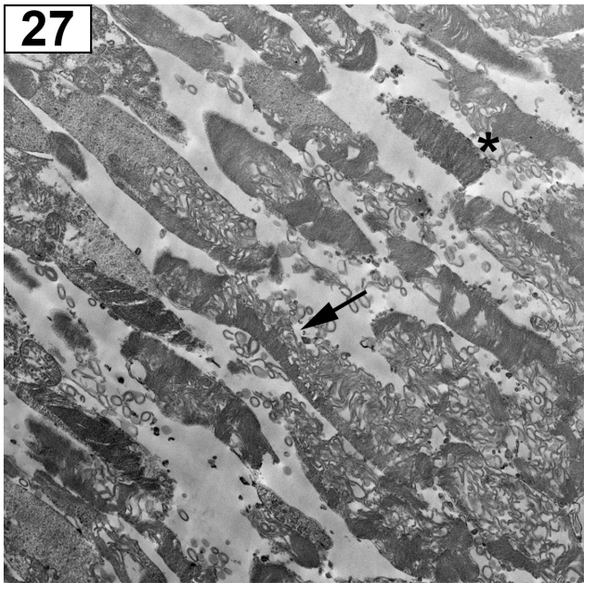

Fig. 27: EM of retina of (GIII) showing outer segments (OS) of photoreceptors with disorganized lamellar discs (*) and some show vesicular dilation (↑).

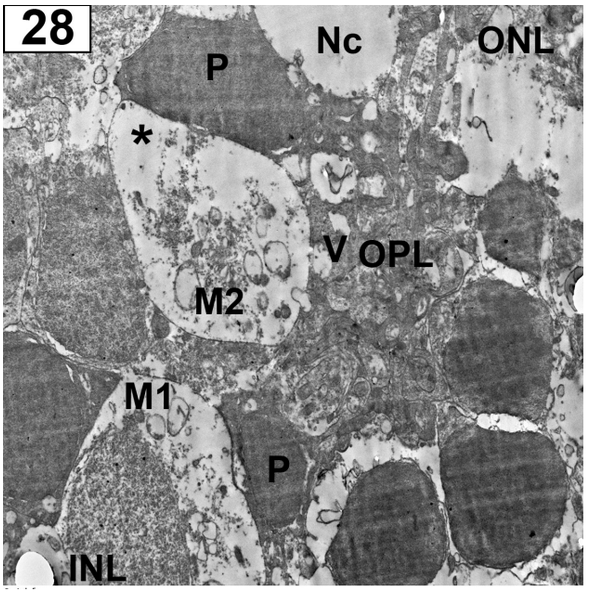

Fig. 28: EM of retina of (GIII) showing distorted ONL with heterochromatic nuclei of its cells with vacuolation between cells. OPL appear distorted with some vacuoles (V). some INL cells appear distorted with destructed mitochondria (M1) and others with heterochromatic nucleus. Markedly necrotic cells (Nc) and remnants of some cells (*) with ballooned mitochondria (M2) in INL are seen.

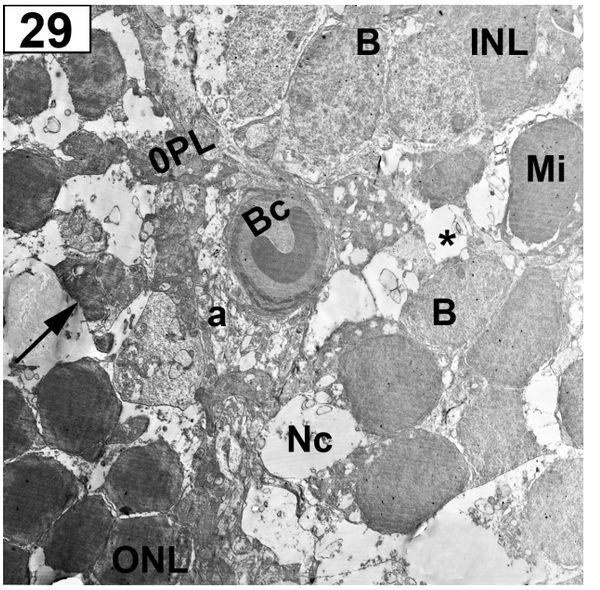

Fig. 29: EM of retina of (GIII) showing distorted ONL with some dense heterochromatic cells (arrow). OPL show congested blood capillary (Bc) and dilated terminal synaptic processes (a). The INL contains bipolar (B), Muller (Mi) and some necrotic cells (Nc) with wide spaces (*) in between the cells.

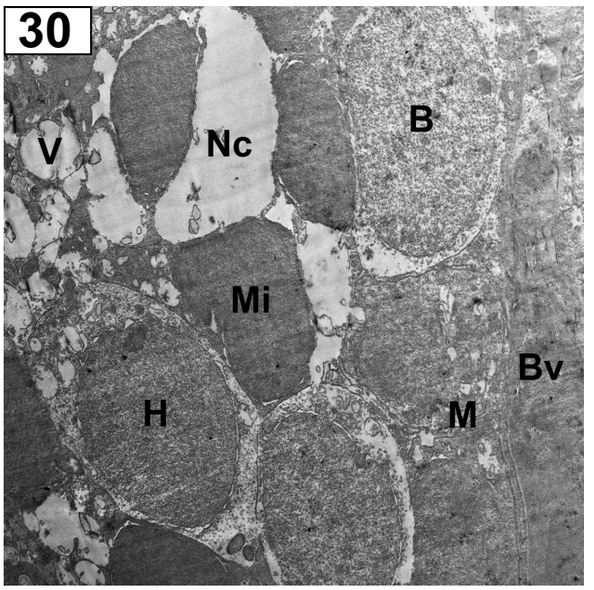

Fig. 30: EM of retina of (GIII) showing shrunken irregular Muller cells (Mi) with loss of its process which apparently increased in number, rarefied cytoplasm of bipolar cells (B) and horizontal cells(H). Multiple vacuolation (V) between cells are seen. Notice: necrotic cell (Nc) is seen

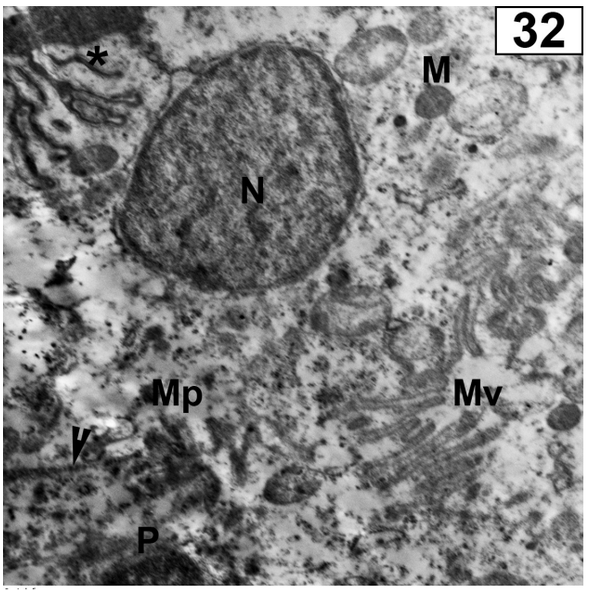

Fig. 32: EM of retina of (GIV) showing retinal pigmented epithelium with rarefied cytoplasm and mitochondria with irregular cristae (M), few melanin pigments (Mp). Basal infoldings (*), apical microvilli (Mv) and intercellular junction (arrow head) are seen. Notice: small pyknotic cell (P) is still seen.

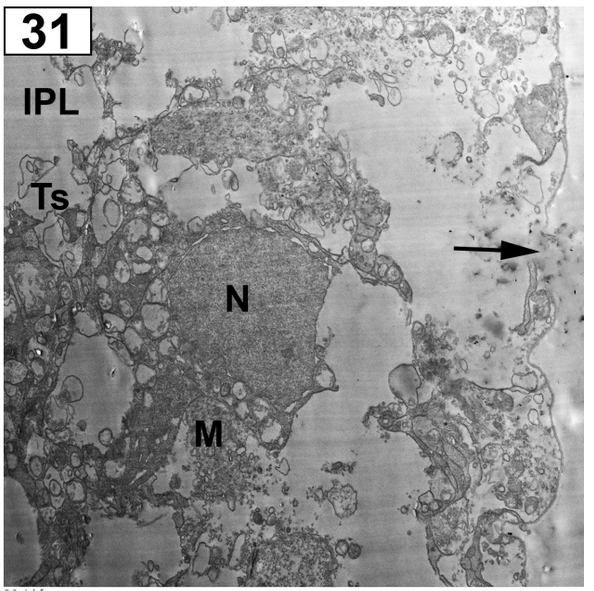

Fig. 31: EM of retina of (GIII) showing irregular ganglion cells with electron dense irregular nucleus (N). The cytoplasm of the cells contains degenerated mitochondria (M). Notice: Distorted dilated terminal synaptic process (Ts) in IPL and damaged distorted inner limiting membrane (arrow).

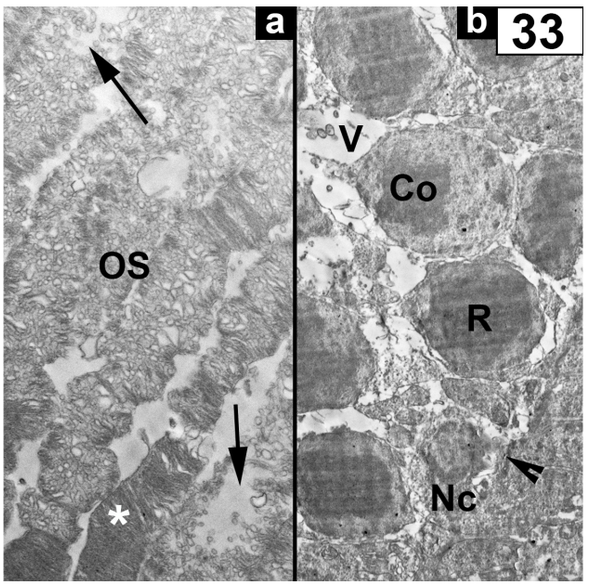

Fig. 33: EM of retina of (GIV) showing (a part) OS of PRL with horizontal lamellar discs in some area (*) and vacuolar degeneration in others (arrows). (b part) Cells of rods (R) and cones (Co) of ONL with some space and vacuoles (V) between them. Inner nuclear membrane (arrow head) and few necrotic cells (Nc) are still seen.

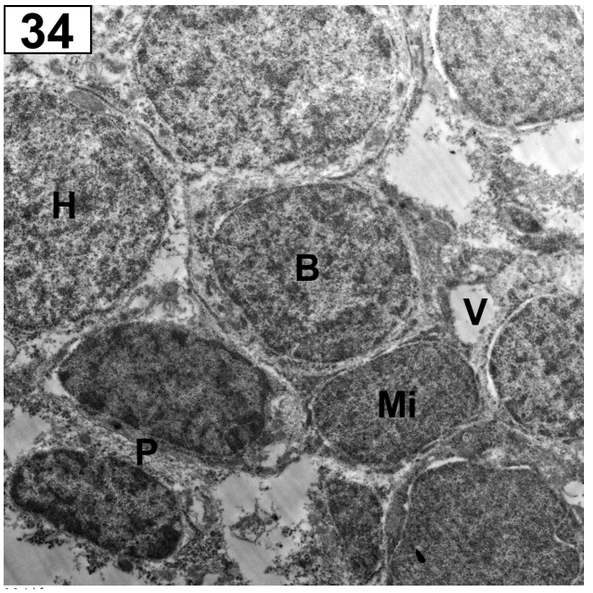

Fig. 34: EM of retina of (GIV) showing INL with muller (Mi), bipolar (B) and horizontal (H) cells. Small shrunken (P) cells and small vacuoles (V) are still seen.

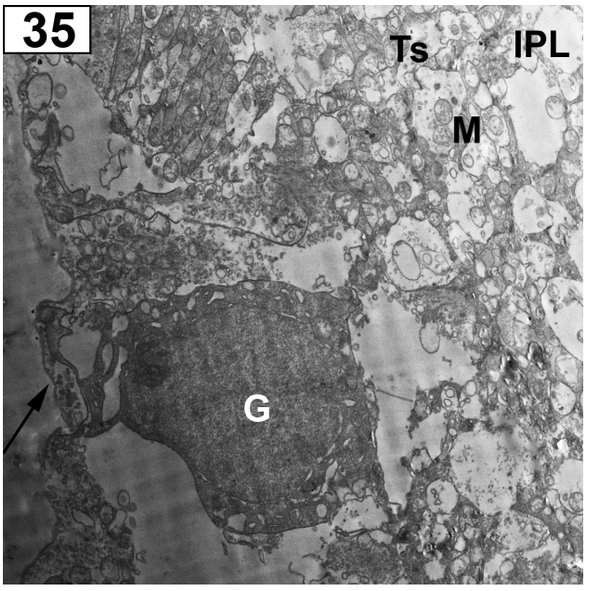

Fig. 35: EM of retina of (GIV) showing ganglion cell(G), dilated terminal synaptic process (Ts) of IPL NOTICE: some mitochondria (M) with irregular cristae and irregular inner limiting membrane (arrow)

Table 1: Mean value ± SD of Retinal layers in all studied groups

Parameters	ONL(µm)	OPL (µm)	INL (µm)	IPL (µm)
I	45.09±2.05	13.65±2.76	32.04±2.01	70.95±7.33
II	47.11±1.65	12.99±3.69	31.63±5.26	74.50±2.17
III	30.89±9.11**	6.33±1.58**	11.79±2.88**	40.51±4.37**
IV	42.01±4.94	10.00±3.99	28.09±2.36	65.98±4.23

* Significant ($p < 0.05$) as compared to Control group.
** highly significant ($p < 0.001$) as compared to Control group.

Table 2: Mean value ± SD of numbers of ganglion cells in all studied groups

group	GROUP I	GROUP II	GROUP III	GROUP IV
Gaglian cells	14.60±2.10	15.20±1.60	3.80±0.40**	11.60±0.80

* Significant ($p < 0.05$) as compared to Control group.
** highly significant ($p < 0.001$) as compared to Control group.

Table 3: Mean value ± SD of intensity of immunostaining in all studied groups

Parameters	GFAP	Caspase 3	INOS
I	2.7±0.68	undetectable	undetectable
II	3.1±0.21	undetectable	undetectable
III	7.89±0.92*	4.00±0.97*	1.060±0.32*
IV	5.43±0.71	2.00±1.25	0.945±0.07

* Significant ($p < 0.05$) as compared to Control group.
** highly significant ($p < 0.001$) as compared to Control group.

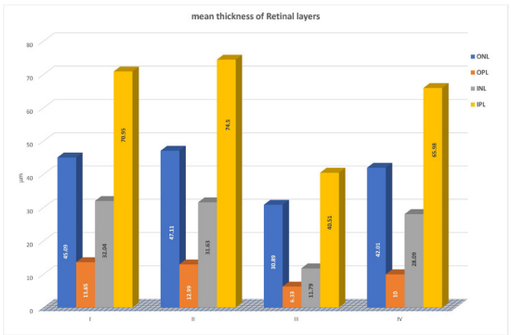

Chart 1: mean thickness of Retinal layers in all studied groups"

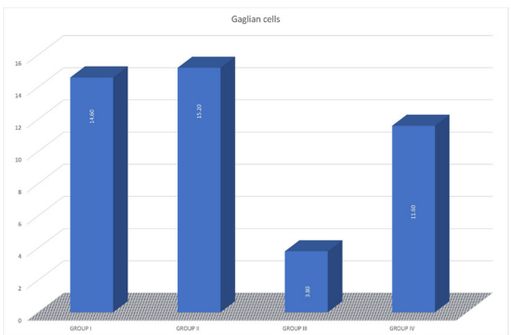

Chart 2: "Mean numbers of Ganglion cells in all studied groups"

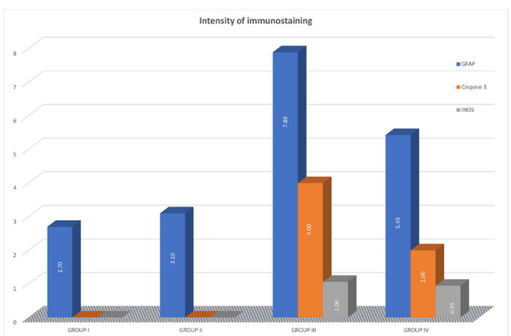

Chart 3: Mean value of immunostaining in all studied groups".

DISCUSSION

Retinal degeneration is a morbid procedure distinguished by loss of vision progressively. Blindness can result from various inherited retinal and retinal-neuronal degenerative diseases such as retinitis pigmentosa and age-related macular degeneration[12].

We used sodium iodate induced retinal damage as the most common model of retinal degeneration. However, its complete mechanisms of action are still unclear[21]. NaIO3 produce retinal degeneration by reactive oxygen species (ROS) production. Severe degeneration might be attributed to the sensitivity of the retina to oxidative stress as it is one of the tissues that have highest oxygen consumption levels in the body[22].

Furthermore, $NaIO_3$ inhibit enzymes activity as triose phosphate dehydrogenase, lactate dehydrogenase and succinyl dehydrogenase in RPE cells and increased conversion of glycine to toxic glyoxylate[7]. In addition, some researches prove that cell death after exposition to $NaIO_3$ may be due to both apoptosis and necrosis[23].

$NaIO_3$ is firstly considered to be specific to RPE cells but recent studies have indicated a direct damaging effect of $NaIO_3$ on RPE and sensory retina[3,7].

The H & E results of $NaIO_3$ group showed cellular infiltration around congested blood capillaries in the choroid, this were in accordance with Moriguchi *et al*.,[10] who explained that by increasing of Il-1b and Il-6 and inflammatory cytokines which are involved in recruitment of macrophages and monocytes from choroid to invade the retina causing retinal cell death and phagocytosis of melanin pigments[24].

H &E stained sections of sodium iodate group (GIII) showed degeneration, loss of retinal pigmented epithelium and disrupted structure of photoreceptor layers, this was in line with Hanus *et al*.,[25]. This could be explained by extensive destruction of the RPE subsequently resulted in progressive degeneration of photoreceptors causing their death. Degeneration of RPE was related to oxidative stress as it contains antioxidant enzymes[25].

Retinal pigment epithelium cells support surrounding cells by paracrine and autocrine growth factors hence promote retinal homeostasis and counteract the cytotoxic effect of different proapoptotic stressors[7]. So, adhesion between the sensory retina and the RPE layer was lost in response to $NaIO_3$ intoxication[3]. Also, detachment of sensory retina from the RPE could be due to huge collection of oxidation stress debris in the subretinal space[4].

Hippert *et al*.[26] added that photoreceptor death lead to disruption the OLM, thinning, disorganization and degeneration of outer nuclear layer and inner nuclear layer this was in harmony with GIII in our study.

Loss of reticular appearance, thinning and deposition of eosinophilic material in outer plexiform layer in GIII were seen. Also, apparent decrease in the synapses in the inner plexiform layer was detected. These were in harmony with Moriguchi, et.al.,[10]. These results were confirmed statistically as there was a highly significant decrease in the thickness of ONL, OPL, INL and IPL in this group as compared to the control group. These results might be attributed to apoptotic death of retinal neurons[24,27].

Group III showed marked vacuolation in ONL, INL, ganglion cell and nerve fibers layers. Ganglion cells were degenerated with pyknotic nuclei. This was in harmony with highly significant decreasing in ganglion cells numbers in morphometric results. Because ganglion cells are most exposed to damage as their axons are rich in mitochondria[3,28]. Also, disrupted and disorganized inner limiting membrane was seen. It might be due to the oxidative stress[29].

In addition, some sections of GIII showed dilation, congestion of blood vessels and hemorrhage in ONL and GCL. This was in accordance with Aplin *et al*.,[22] who explained that as a compensatory change occurring in the capillaries. A decrease in capillary stability reduce its ability to meet the metabolic needs and the resulting is loss of most layers of retina[3].

Congested blood vessels could be explained by the inflammatory process occurred due to making of pro-inflammatory mediators as tumor necrosis factor-α (TNF-α), interleukin-1 (IL-1) by the reactive glial cells; Muller cells and microglia. Furthermore, ROS might lead to lesion of blood-retinal barrier with subsequent invasion of small blood vessels to the sub-retinal space. These blood vessels might break and/or leak resulting into hemorrhage as seen in G III[26].

Sections of (GIII) showed strong positive immune reaction of GFAP of Muller cells in INL with extension of thick processes to IPL. Strong positive reaction of astrocytes in GCL and NFL especially around blood vessels was seen. These were in agreements with Aplin *et al*.,[22] who stated that Muller cell gliosis appeared strongest in degenerating areas after $NaIO_3$. Also, they proved that astrocytes activation in NFL and GCL was common in degeneration processes[22]. These results confirmed by morphometric results.

Also, Mohamed *et al*.,[29] added that Muller cell gliosis is a complicated process that result in progressive neuronal loss. A hallmark of gliosis is the elevation of glial fibrillary acidic protein as seen in GIII[27].

Muller cells, the main retinal glial cells were extensively stimulated by severe retinal injury to proliferate and migrate invading the areas of lesions in all retinal layers and surrounding the entire retina by forming subretinal glial tissue. Such subretinal gliosis might aggravate the retinal lesion by blocking the blood supply from the choroid to the outer retina[24].

Furthermore, the conversion of glutamate to glutamine by affected Muller cells was decreased. So, glutamate accumulates to high levels leading to uncontrolled entrance of calcium ions intracellular causing neurotoxicity[27].

In our study GIII showed strong positive cytoplasmic reaction for caspase-3 in cells of ONL, INL and GCL due to apoptosis. These results were confirmed statistically as a significant increase in area percentage for caspase-3 in this group as compared to the control. These were in harmony with other researches who confirmed strong reaction of caspase-3 immunostaining in many layers of retina due to apoptosis caused by $NaIo_3$[3,5,30].

Strong positive iNOS immunostaining in all layers of retina was seen in GIII, this was in harmonization with Liu *et al*.,[5] who explained that with necrosis caused by $NaIo_3$. Necrosis produce cytokines as (TNF-α) which stimulate Muller and microglia cells to produce inducible iNOS[31]. Increased iNOS led to increase production of nitric oxide, a reactive radical gas, resulting into more damage of the tissues by reactive nitrogen species[24]. These results confirmed by morphometric results which showed significant increase in iNOS expression due to necrosis by $NaIo_3$.

Ultrastructurally, the retinal pigment epithelium of group III showed destructed basal infoldings, vacuolated cytoplasm, damaged mitochondria and distorted microvilli. These were matching with other studies[3,27] which confirmed damage of different organelles in retinal cells due to oxidative stress by $NaIo_3$.

Hanus J, et. al[25] added that destruction of the tight junctions between RPE cells (blood–retinal barrier) was noticed due to degradation of ZO-1 protein after $NaIO_3$ administration as in GIII in this study.

Photoreceptor outer segments showed disorganization and vesicular dilation of lamellar discs. These were reported by Mohamed *et al*.,[29] who linked these changes to the effect of oxidative stress.

In the present work, the outer nuclear layer of GIII showed vacuolation and hyperchromatic nuclei. OPL containing congested dilated blood vessel and cystic dilatation of terminal synaptic processes and damaged mitochondria were seen. INL showed vacuolation between cells, bipolar cells with rarefied cytoplasm and destructed mitochondria and heterochromatic irregular Muller cells with loss of its processes and apparent increase in its number. Similar findings were observed by Caro-Ordieres *et al*.,[31] and Czarnik-Kwaśniak et, al.[32] who explained that damage by oxidative stress.

In GIII, inner plexiform layer presented with distorted terminal synaptic process. This was in line with Alsaeedi and coworkers[2] who added that connectivity between photoreceptors, bipolar cell processes and ganglion cells were lost over some areas. Furthermore, ganglion cells in GIII showed heterochromatic irregular nuclei, dilated RER and destructed mitochondria as it has high sensitivity to oxidation stress[2].

Silymarin has effective antioxidant properties through scavenging free radicals and increasing endogenous antioxidant defenses such as intracellular glutathione (GSH) and decreasing apoptotic cell death[22].

H&E stained sections of group IV showed marked improvement of histological picture and appearance of all layers of retina but some vacuolation in ONL and INL and some cells in IPL were still seen. This were in agreement with Xie *et al*.,[33] who explained this by antioxidant effects of silymarin by reducing both lipid and protein oxidation as well as by activating acetylcholinesterase activity.

GFAP immunostaining of GIV revealed positive immune reaction of astrocyte of GCL &NFL and weak reaction of Muller cells in ONL and extension of thin processes to OPL. This decreasing in stain intensity as compared to GIII harmonized with Vargas-Mendoza

et al.,[14] who explained this by inhibition of NF-jB activation as well as other inflammatory mediators.

Sections of GIV revealed moderate immunoreactivity of caspase 3 in GCL only. This was in accordance with Shen *et al*.,[34] due to it antiapoptotic effects of Silymarin.

GIV showed moderate immunoreactivity of iNOS in GCL only. This was in accordance with Vargas-Mendoza *et al*.,[14] who explained that by silymarin reduced nitro tyrosine level. Morphometric results of GIV were in harmonization with light results.

EM sections of retina of GIV showed marked improvement but some disorganized lamellar discs of OS and few damaged mitochondria of retinal cells were seen. Few necrotic and pyknotic cells with minimal intercellular spacing in both ONL and INL were noticed. These were in line with Huilgol and Jamadar[35], Petrásková *et al*.,[36] who explained that silymarin stimulates DNA-dependent RNA polymerase, leading to increased protein synthesis and thus promoting healing and reparative processes.

In conclusion, the $NaIO_3$ pattern of retinal degeneration supply a compound process of different cell-death pathways and affecting both RPE and neurosensory retina. Therefore, it should serve as the model of choice for the investigation of the efficiency of different therapy. Silymarin is effective flavonoids that ameliorate the denegation of all retina layers. Silymarin has a promising role in prevention many degenerative retinal diseases.

CONFLICT OF INTERESTS

There are no conflicts of interest.

REFERENCES

1. El Ebiary FHK, Mekawy MAEA, Abd El Samad AA and Negm EA: Mesenchymal stem cells as a possible therapy in experimentally induced retinal damage in Albino rat: Histological study. EJH, (2018); Article 8, 41(3): 329-344.
2. Alsaeedi HA, Koh AE, Lam C, Abd Rashid MB, Harun MHN, Saleh MF, The SW, Luu CD, Ng MH, Isa HM, Leow SN, Then KY, Bastion MC, Mok PL, Muthuvenkatachalam BS, Samrot AV, Swamy KB, Nandakumar J and Kumar SS: Dental pulp stem cells therapy overcome photoreceptor cell death and protects the retina in a rat model of sodium iodate-induced retinal degeneration. J Photochem Photobiol B. (2019); 198: 111561.
3. Balmer J, Zulliger R, Roberti S and Enzmann V: Retinal Cell Death Caused by Sodium Iodate Involves Multiple Caspase-Dependent and Caspase-Independent Cell-Death Pathways. Int J Mol Sci. (2015); 16(7):15086-103.
4. Kim H, Nam SM, Chang B, Nahm S and Lee J: Ultrastructural Changes and Expression of PCNA and RPE65 in Sodium Iodate-Induced Acute Retinal Pigment Epithelium Degeneration Model. Neurochem Res. (2018); 43(5): 1010-1019.
5. Liu Y, Li Y, Wang C, Zhang Y and Su G: Morphologic and histopathologic change of sodium iodate-induced retinal degeneration in adult rats. Int J Clin Exp Pathol. (2019); 12(2): 443-454.
6. Sadamoto K, Yamagiwa Y, Sakaki H and Kurata M: Absence of histopathological changes in the retina of zebrafish treated with sodium iodate. J Vet Med Sci. (2018); 80 (6): 901-908.
7. Huang J, Liu Y, Mao K, Gu Q and Wu X: Tetramethylpyrazine protects mice retinas against sodium iodate-induced oxidative injury. Mol Vis. (2020); 26: 494-504.
8. Kadkhodaeian HA, Tiraihi T, Daftarian N, Ahmadieh H, Ziaei H and Taheri T: Histological and Electrophysiological Changes in the Retinal Pigment Epithelium after Injection of Sodium Iodate in the Orbital Venus Plexus of Pigmented Rats. J Ophthalmic Vis Res. (2016); 11(1): 70–77.
9. Du W, An Y, He X, Zhang D and He W: Protection of Kaempferol on Oxidative Stress-Induced Retinal Pigment Epithelial Cell Damage. Oxidative Medicine and Cellular Longevity. (2018); Article ID 1610751.
10. Moriguchi M, Nakamura S, Inoue Y, Nishinaka A, Nakamura M, Shimazawa M Hara H: Irreversible Photoreceptors and RPE Cells Damage by Intravenous Sodium Iodate in Mice Is Related to Macrophage Accumulation. Invest Ophthalmol Vis Sci. (2018); 59(8): 3476-3487.
11. Nadal-Nicolas FM and Patricia Becerra S: Pigment Epithelium-derived Factor Protects Retinal Pigment Epithelial Cells Against Cytotoxicity "In *Vitro*". Adv Exp Med Biol. (2018); 1074: 457–464.
12. Liu Y, Li R, Xie J, Hu J, Huang X, Ren F and Li L: Protective Effect of Hydrogen on Sodium Iodate-Induced Age-Related Macular Degeneration in Mice. Front Aging Neurosci. (2018); 10: 389.
13. Shiri S, Abbasi N, Alizadeh K and Karimi E: Preventive effects of silymarin in retinal intoxication with methanol in rat: Novel and green synthesis of a nanopolymer and its use as a drug delivery system of silibinin and silymarin extracts in the olfactory ensheathing cells of rats in normal and high-glucose conditions. RSC ADVANCES. (2019); 9 (67): 38912-38927.
14. Vargas-Mendoza N, Morales-González Á, Morales-Martínez M, Soriano-Ursúa MA, Delgado-Olivares L, Sandoval-Gallegos EM, Madrigal-Bujaidar E, Álvarez-González I, Madrigal-Santillán E, Morales-Gonzalez JA: Flavolignans from Silymarin as Nrf2 Bioactivators and Their Therapeutic Applications. Biomedicines. (2020); 8(5):122.

15. Xiao J, Yao J, Jia L, Lin C and Zacks DN: Protective Effect of Met12, a Small Peptide Inhibitor of Fas, on the Retinal Pigment Epithelium and Photoreceptor After Sodium Iodate Injury. Invest Ophthalmol Vis Sci. (2017); 58(3):1801-1810.

16. Kiernan JA. (2015). Histological and histochemical methods; theory and practice. pp. 238–310. 5th ed, Scion Publishing Ltd, Banbury, UK

17. Suvarna K, Layton C and Bancroft j: Bancroft's Theory and Practice of Histological Techniques. Elsevier. (2018); 8th ed.: 408-418.

18. Ramos-Vara JA, Kiupel M, Baszler T, Bliven L, Brodersen B, Chelack B, Czub S, Del Piero F, Dial S, Ehrhart EJ, Graham T, Manning L, Paulsen D, Valli VE and West k: Suggested guidelines for immunohistochemical techniques in veterinary diagnostic laboratories. J Vet Diagn Invest. (2008); 20(4):393-413.

19. Bozzola JJ: Conventional specimen preparation techniques for transmission electron microscopy of cultured cells. Methods Mol Biol. (2014); 1117:1-19.

20. Dawson B and Trapp RG: Basic and clinical biostatistics. 5th ed. New York: McGraw-Hill Education / Medical; (2020).

21. Chan C, Huang D, Sekar P, Hsu S and Lin W: Reactive oxygen species-dependent mitochondrial dynamics and autophagy confer protective effects in retinal pigment epithelial cells against sodium iodate-induced cell death. J Biomed Sci. (2019); 26: 40.

22. Aplin FP, Vessey KA, Luu CD, Guymer RH, Shepherd RK and Fletcher EL: Retinal Changes in an ATP-Induced Model of Retinal Degeneration. Front Neuroanat. (2016); 10: 46.

23. Zhang J, Zhao X, Cai Y, Li Y, Yu X and Lu L: Protection of Retina by Mini-αA in NaIo3-Induced Retinal Pigment Epithelium Degeneration Mice. Int J Mol Sci. (2015); 16(1): 1644–1656.

24. Farag E, Yousry MM and Omar AI: Histological study on the detrimental influences of white LED light on the retina of adult albino rat and the potential effect of simultaneous nicotine administration with highlighting their possible mechanisms. EJH. (2017); 40(3):328-344.

25. Hanus J, Anderson C, Sarraf D, Ma J and Wang S: Retinal pigment epithelial cell necroptosis in response to sodium iodate. Cell Death Discov. (2016); 2: 16054.

26. Hippert C, Graca AB, Barber AC, West EL, Smith AJ, Ali RR and Pearson RA: Müller Glia Activation in Response to Inherited Retinal Degeneration Is Highly Varied and Disease-Specific. PLoS One. (2015); 10(3): e0120415.

27. Gawish MF, Mazen NF; Hassen EZ and Adbelhady ME: Light and Electron Microscopic Study on the Possible Ameliorative Role of Adipose-Derived Mesenchymal Stem Cells on Diabetic Retinopathy in Adult Male Albino Rats. EJH. (2018); 41(4): 582-596.

28. Yang Y, Qin YJ, Yip YWY, Chan KP, Chu KO, Chu WK, Ng TK, Pang CP and Chan SO: Green tea catechins are potent anti-oxidants that ameliorate sodium iodate-induced retinal degeneration in rats. Sci Rep. (2016); 6: 29546.

29. Mohamed MEI, El-Shaarawy EAA, Youakim MF, Shuaib DMA and Ahmed MM: Aging changes in the retina of male albino rat: a histological, ultrastructural and immunohistochemical study. Folia Morphol (Warsz). (2019); 78(2): 237-258.

30. Fan J, Shen W, Lee SR, Mathai AE, Zhang R, Xu G, Gillies MC: Targeting the Notch and TGF-β signaling pathways to prevent retinal fibrosis in *vitro* and in *vivo*. Theranostics. (2020); 10(18):7956-7973.

31. Caro-Ordieres T, Marín-Royo G, Opazo-Ríos L, Jiménez-Castilla L, Moreno JA, Gómez-Guerrero C, Egido J: The Coming Age of Flavonoids in the Treatment of Diabetic Complications. J Clin Med. (2020); 9(2):346.

32. Czarnik-Kwaśniak J, Kwaśniak K, Kwasek P, Świerzowska E, Strojewska A, Tabarkiewicz J. The Influence of Lycopene, [6]-Gingerol, and Silymarin on the Apoptosis on U-118MG Glioblastoma Cells In *Vitro* Model. Nutrients. 2019 Dec 30;12(1):96.

33. Xie Y, Zhang D, Zhang J and Yuan J: Metabolism, Transport and Drug-Drug Interactions of Silymarin. Molecules. (2019); 24(20):3693.

34. Shen Y, Zhao H, Wang Z, Guan W, Kang X, Tai X and Sun Y. Silibinin declines blue light-induced apoptosis and inflammation through MEK/ERK/CREB of retinal ganglion cells. Artif Cells Nanomed Biotechnol. (2019); 47(1): 4059-4065.

35. Huilgol SV and Jamadar MG: Silymarin, an antioxidant bioflavonoid, inhibits experimentally-induced peptic ulcers in rats by dual mechanisms. Int J Appl Basic Med Res. (2012); 2(1): 63–66.

36. Petrásková L, Káňová K, Biedermann D, Křen V and Valentová K: Simple and Rapid HPLC Separation and Quantification of Flavonoid, Flavonolignans, and 2,3-DehydroflaviNOS onolignans in Silymarin. Foods. (2020); 9(2):116.

الملخص العربى

دراسة هستولوجية و هستوكيميائية لتأثير مادة أيودات الصوديوم علي شبكيه العين لذكر الفأر الأبيض البالغ و الدور الوقائي المحتمل لعقار السيملارين

رانيا إبراهيم ياسين[١]، أميمة إبراهيم زيدان[٢]، نجوى سعد غنيم[١]

[١]قسم هيستولوجيا وبيولوجيا الخلية، [٢]قسم قسم التشريح، كلية الطب، جامعة المنوفية

المقدمه: تنتج امراض تلف شبكيه العين من عوامل بيئيه و جينيه مختلفه والتي قد تؤدي الي العمي الدائم و تستخدم ماده ايودات الصوديوم علي نطاق واسع في اتلاف نسيج الشبكيه لدراسه ميكانيكيه تلف الخلايا بها .عقار السيميلارين له تأثير قوي كمضاد للأكسده .

الهدف من البحث: دراسه التأثير الضار لماده ايودات الصوديوم علي شبكيه العين لذكر الفأر الأبيض البالغ و الدور الوقائي المحتمل لعقار السيميلارين .

خطوات و طرق البحث: استخدم اربعون من ذكور الفئران البيضاء البالغه و قسمت الي اربعه مجموعات متساويه , المجموعه الاولي (ضابطه) , المجموعه الثانيه (تناولت عقار السيميلارين) , المجموعه الثالثه (حقنت بماده ايودات الصوديوم) , المجموعه الرابعه (تناولت عقار السيميلارين ثم حقنت بماده ايودات الصوديوم) في نهايه التجربه اخذت عينات من شبكيه العين من جميع المجموعات و جهزت للفحص الهستولوجي الضوئي و المجهري و صبغت شرائح البارافين بصبغه الهيماتوكسيلين و الأيوسين و صبغات جيفاب و كاسباز و اكسيد النيتريك سينسيز المستحث المناعيه .

نتيجه البحث: اظهرت صبغه الهيماتوكسيلين و الأيوسين للمجموعه الثالثه نقص واضح في سمك الشبكيه و اعتلال و فقد لكثير من الطبقات المكونه لها و تلف في طبقه الخلايا الطلائيه الملونه و مستقبلات الضوء و تلف و فقد في خلايا طبقتي الأنويه الداخليه و الخارجيه و كذلك خلايا العقد العصبيه و نقص في سمك و فقد للشكل الشبكي لطبقتي الضفيره الداخليه و الخارجيه و احتقان في كثير من الأوعيه الدمويه و زياده ملحوظه في صبغات جيفاب و كاسباز و اكسيد النيتريك سينسيز المستحث المناعيه , و اظهرت نتائج المجموعه الرابعه تحسن واضح في التركيب الهستولوجي لطبقات شبكيه العين مع وجود بعض التجاويف , و قد اكدت النتائج الاحصائيه و نتائج الميكروسكوب الالكتروني ما اظهره الميكروسكوب الضوئي كما لوحظ نقص في الصبغات المناعيه .

الاستنتاج: ماده ايودات الصوديوم لها تاثير مدمر لكل طبقات الشبكيه و ماده السيميلارين لها دور وقائي كبير .